Effect of drug-binding-induced deformation on the vibrational spectrum of a DNA·daunomycin complex

Y. Z. Chen,[1,2] A. Szabó,[2] D. F. Schroeter,[3] J. W. Powell,[3] S. A. Lee,[2] and E. W. Prohofsky[1]
[1]*Department of Physics, Purdue University, West Lafayette, Indiana 47907-1396*
[2]*Department of Physics and Astronomy, University of Toledo, Toledo, Ohio 43606*
[3]*Department of Physics, Reed College, Portland, Oregon 97202*
(Received 19 February 1997)

Vibrational frequencies of a DNA·daunomycin complex and those of a free DNA helix and an isolated daunomycin are calculated and compared with the infrared spectrum of similar systems at frequencies above 600 cm^{-1}. Our study indicates that the binding induces a considerable change in the vibrational spectrum of both DNA and the binding drug. The frequency shifts appear to be closely related to the conformational deformation in the complex caused by drug binding. Significant frequency shift is found in the normal modes in the DNA·drug complex that are primarily vibrations localized to the sugar-phosphate backbone of the binding site. Sizable frequency change is also found in the modes associated with base atoms involved in the drug binding and in the modes in regions of the binding daunomycin that are deformed by the binding. In contrast the frequency of the modes in the region with no significant deformation is relatively unchanged. The modification of the DNA dynamical force field by the nonbonded interactions between DNA and the drug is found to have little effect on the modes in DNA above 600 cm^{-1}. The modification to the daunomycin dynamical force field appears to be sizable since the frequency of several daunomycin modes is changed by several cm^{-1}. The close relationship between structure and spectrum revealed in this work is of potential application in the identification of sites and types of deformation of a biomolecule from Raman and infrared spectra. [S1063-651X(97)08906-X]

PACS number(s): 87.15.He, 87.64.Je, 87.15.Kg, 87.15.By

INTRODUCTION

The advantage of vibrational spectroscopy in the study of structure as well as dynamics of biomolecules is well established [1,2]. The applicability of Raman and infrared (IR) spectroscopy on biomolecules of different sizes and over a wide range of conditions such as the state of sample (liquid, disordered solid, or crystal), temperature, and *p*H facilitates their use in the study of many biologically important processes and structural transitions that are inaccessible to other techniques. The observed spectra combined with theoretical computations yield structure-relevant spectroscopic features of biomolecules. High frequency modes correspond to highly localized vibrational motions. The knowledge of the structural feature of these modes can then be used to analyze and interpret the spectrum to yield information about the sites of binding and types of deformation in these molecules.

A number of theoretical and experimental studies have been carried out that examine the correlation between the structure and vibrational spectrum in DNA. Computational analyses have revealed the existence of structurally sensitive vibrational modes in different conformations of DNA [3–5]. Conformationally sensitive IR [1] and Raman bands [2,6–9] in DNA *A*, *B*, and *Z* families have also been identified experimentally. Several studies were carried out to compare Raman spectra from samples in solution and those in crystals [8–10].

Recently we have carried out a theoretical calculation [11] to determine the vibrational spectrum of a netropsin drug-DNA complex and compared this with our observed Raman and IR spectra of similar systems [12] at frequencies above 600 cm^{-1}. Our study further showed that the vibrational spectrum in this frequency range is highly sensitive to the structural deformation resulting from the drug binding. A substantial frequency shift was found in the normal modes that are primarily localized in the regions of the binding netropsin where significant structural deformation occurs. On the other hand, the frequencies of the normal modes primarily localized in the rest of the drug-DNA complex are relatively unchanged in agreement with the observation from x-ray crystal studies that no significant structural deformation occurs in this part of the complex. The forces between DNA and the binding netropsin were found to have little effect on the normal modes in the high frequency region. Therefore our earlier study revealed a close relationship between structure and high frequency spectrum.

In the present work we report a combined theoretical and experimental study of the vibrational properties of DNA, daunomycin, and the DNA·daunomycin complex. We focus our attention on the modes in the frequency range above 600 cm^{-1}. This choice is made because it is easier to obtain high precision experimental frequencies in this frequency range. In addition the modes in this frequency range are less affected by nonbonded force fields for which only crude models are available. Daunomycin is an anthracycline antibiotic drug widely used in the treatment of various cancer diseases. Daunomycin has a chemical structure (see Fig. 1) that allows a twofold binding mechanism to DNA: intercalation and groove binding. The intercalation is afforded by the heterocycle part of its structure (labeled ''aglycon'' in Fig. 1) and

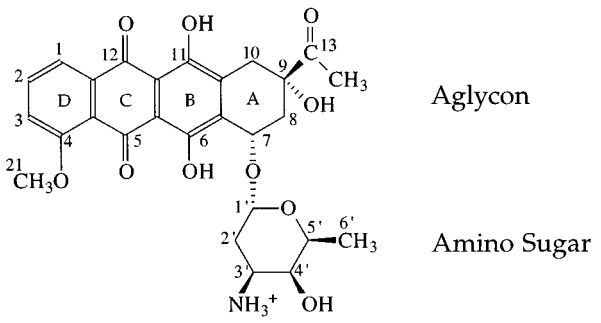

FIG. 1. Chemical structure of daunomycin.

the groove binding occurs because the single amino sugar ring lies in the minor groove in the complex and acts as the donor for hydrogen bonds to the phosphate groups of the DNA backbone. Daunomycin is known to inhibit both DNA replication and RNA transcription [13]. As a paradigm of anticancer intercalating drugs, daunomycin and DNA·daunomycin systems have been extensively studied by a variety of techniques including crystallographic structural analyses [14–18], thermodynamic measurements [19–21], and theoretical investigations [22–25]. The structural and dynamical information provided by these studies can be utilized to analyze the structural features of the vibrational spectrum of DNA·daunomycin complexes.

The intercalation of the aglycon planar group into the space between base pairs displaces and unwinds the adjacent base pairs primarily through changes in individual torsion angles in the local sugar-phosphate groups at the binding site. Although these torsion angles generally fall in the region of a *B*-type DNA conformation, the deformation is sufficiently large to accommodate the drug molecule. As a result the conformation of the backbone is different from that of *B*-DNA. The significant and numerous structural variations in the backbone are expected to induce changes in the frequency of modes associated with localized vibrational motion in the region. We will show that this is indeed the case. X-ray crystallography [17] has shown that in daunomycin bound DNA the $N2$ and $N3$ atoms of a guanine base adjacent to the drug are involved in direct hydrogen bonding with the drug. A sizable frequency shift is indeed found in the modes associated with these atoms. Such a finding suggests that the vibrational spectrum is also of use in the identification of sites of molecule-ligand bonds.

Binding to DNA is known to induce conformational deformation in certain regions of daunomycin. This deformation is expected to be reflected in the daunomycin modes. Although our calculation is limited by the unrefined daunomycin force constants, we are able to make a qualitative assignment to the daunomycin modes on the basis of frequency shift. These assignments are then used to interpret the observed IR frequency shift for the daunomycin modes. We will show that a sizable frequency shift is found in the modes associated with localized motions in regions that are deformed by the binding. Nonbonded interactions between the drug and DNA have little effect on the DNA modes above 600 cm^{-1}. It, however, does have an effect on the dynamical force field of the daunomycin confined inside DNA, which in turn contributes to a frequency shift in several daunomycin modes of several cm^{-1}.

THEORETICAL METHODS

The DNA polymer considered in this work is a poly d(CGTA)·poly d(TACG), which is an infinitely long double helix with a four-base-pair repeating sequence of CGTA on one strand (C, G, T, and A refer to cytosine, guanine, thymine, and adenine, respectively). The coordinates of the free DNA polymer are generated from fiber data using the helical symmetry of the standard *B* conformation [26]. The coordinates of the daunomycin bound poly d(CGTA)·poly d(TACG) are generated from the crystal x-ray coordinates of a daunomycin·d(CGTACG) complex [16]. In our model of the daunomycin-bound DNA polymer there is one daunomycin drug bound to every section of CGTA sequence. These sections are then connected by helical symmetry with a per unit cell helical rise of 15.7 Å and twist angle of 136°. Such a drug-DNA complex has a drug-base pair ratio of 4 bp/drug. The coordinates of isolated daunomycin are from crystal x-ray data [14].

The helical symmetry in both the drug-free and drug-bound DNA polymers can be used to reduce the calculation of these infinite polymers to the dimensionality of a single unit cell, which contains only four base pairs plus a bound daunomycin for the drug-bound polymer. This reduction in spatial description is achieved by transforming the Hamiltonian into phase (momentum) space. The number of atoms (excluding the hydrogen atoms whose masses and charges are added to their parent atoms) in a unit cell for the two polymers are 164 and 205, respectively. The dimensionality of the equation of motion in phase space is therefore 492 $\times$492 and 615$\times$615, respectively. There are 38 heavy atoms in daunomycin and the dimensionality of the equation of motion for the drug is 114$\times$114.

In internal coordinates the Hamiltonian of a harmonic system with helical symmetry is given by

$$H=\sum_{n,i}\frac{1}{2}M_i\dot{\mathbf{u}}_{ni}^2+\sum_k\sum_{n,m}\sum_j\frac{1}{2}\phi_{n-m,j,k}s_{n-m,j,k}^2 \quad (1)$$

where n and m are the indices of unit cells, i is the index of the atoms in a unit cell, j is the index for internal coordinates, and k specifies the types of harmonic motion (valence bond stretch, angle bending, torsion, out-of-plane bending, H bonding, and motions induced by the nonbonded atom-atom van der Waals and Coulomb interactions). $\mathbf{u}_{ni}$ is the displacement of the ith atom in the nth unit cell in Cartesian coordinates, $s_{n-m,j,k}$ is the internal coordinate, and $\phi_{n-m,j,k}$ is the effective internal force constant for a particular bond motion. The force constants include a standard valence force field, hydrogen bond force constants, and a nonbonded force field including van der Waals and Coulomb interactions. These force constants are dependent on the separation of units. The detailed description of the force fields for the atoms in DNA can be found in our earlier publication [11]. The same set of valence force constants are used for both free and daunomycin-bound DNA. The valence force constants of daunomycin are from AMBER [23], a biomolecular mechanics and dynamics simulation software package. The drug-base H-bond force constants were determined in an earlier work [24]. The nonbonded Coulomb and van der Waals force constants between the drug and DNA atoms are the same as that used in our earlier study of DNA and DNA ·daunomycin systems [24]. The charges of daunomycin atoms are from AMBER [23].

The Hamiltonian in Eq. (1) can be reduced in dimensionality by transformation to a mass weighted Cartesian (MWC) coordinate system, followed by a Fourier transformation into phase (momentum) space. In matrix form this Hamiltonian can be given by

$$H=\int_{-\pi}^{\pi}\frac{1}{2}\left[X^{\dagger}(\theta)\dot{X}(\theta)+\frac{1}{2}X^{+}(\theta)\times\left(\sum_{k}B_{k}^{+}(\theta)\Phi_{k}(\theta)B_{k}(\theta)\right)X(\theta)\right]d\theta, \qquad (2)$$

where $\Phi_k(\theta)$, $B_k(\theta)$, and $X(\theta)$ are the force constant matrix, transformation matrix (B matrix), and the MWC coordinate matrix, respectively, as defined in our earlier publication [24]. θ is the phase difference between adjacent unit cells. The vibrational amplitude in a unit cell is linked to that of the neighboring cell by a factor $e^{-i\theta}$. From Eq. (2) we obtain an equation of motion for our linear helical molecule:

$$\left(\sum_{k}B_{k}^{+}(\theta)\Phi_{k}(\theta)B_{k}(\theta)-\omega_{\lambda}(\theta)^{2}I\right)q^{\lambda}(\theta)=0, \qquad (3)$$

where $\omega_\lambda(\theta)$ and $q(\theta)$ are the eigenfrequency and eigenvector in MWC coordinates, respectively.

For a free daunomycin drug there is only a single unit cell; its equation of motion is thus

$$\left(\sum_{k}b_{k}^{+}\phi_{k}b_{k}-\omega_{\sigma}I\right)q^{\sigma}=0, \qquad (4)$$

where σ is the index of the normal modes, k specifies the type of displacement (valence stretch, angle bending, torsion, out-of-plane bending, and nonbonded van der Waals and Coulomb atom-atom interactions). ω_σ and q^σ are the eigenfrequency and eigenvector in MWC coordinates, respectively. b_k is the transition matrix (B matrix) of a particular displacement from MWC coordinates to internal coordinates.

The formulation of the B matrix for bond stretch, angle bending, torsion, and out-of-plane bending can be found in the literature [27]. The formulation of the B matrix for harmonic motion associated with nonbonded atom-atom interactions is the same as that for the valence bond stretch. ϕ_k is the matrix of force field of the drug divided by the square root of the masses.

The actual computation of the eigenfrequencies and eigenvectors of Eq. (3) and Eq. (4) were carried out on an IBM RS-6000 computer using the IMSL complex Hermitian diagonalization routine DEVCHF.

The assignment of theoretical modes to experimental frequencies is difficult for large molecules. Large molecules have a large number of normal modes and one is faced with a group of theoretical frequencies near each experimental line. As a result, it is difficult to pair modes to particular experimental lines without accurately refined force constants. The initial choice of force constants, determined from different molecules, are not accurate enough in the combined system. It is only after assignment and further refinement of force constants that the assigned frequencies agree. The usual approach to the assignment ambiguity is to do experimental spectral analysis and theoretical mode analysis on isotopically substituted samples. The assignments for the combined system are then made by comparing the shift in frequency for modes sensitive to the isotopic substitution.

The refinement of force constants has previously been carried out for the free DNA helix [3,28] and the assignment is relatively straightforward using these refined force constants. No mode assignment and force constant refinement has been done for the isolated daunomycin and only unrefined initial force constants are available. In an attempt to circumvent the need for isotopically substituted data we make assignments of daunomycin modes on the basis of the agreement between calculated and observed shift in frequency on binding to the DNA. The association with DNA takes the place of isotopic substitution. A sensible assignment scheme results and we can assign modes, both in DNA and in daunomycin, for both the free molecules and the drug-DNA complex.

The assignment of the character of a normal mode for the drug-free and drug-bound polymers can be made by comparing the distribution of potential energy of individual internal motions in the mode. This distribution is approximated by the function $V_{jk}^{\lambda}(\theta)$:

$$V_{jk}^{\lambda}(\theta)=\frac{[s_{jk}^{\lambda}(\theta)]^{*}\Phi_{jk}(\theta)s_{jk}^{\lambda}(\theta)}{\sum_{k}\sum_{j}[s_{jk}^{\lambda}(\theta)]^{*}\Phi_{jk}(\theta)s_{jk}^{\lambda}(\theta)}. \qquad (5)$$

This function is called the potential energy distribution (PED) function. In Eq. (5) j is the index of the internal coordinates, k specifies the types of harmonic motion and λ is the index for the eigenfrequencies. $\Phi_{jk}(\theta)$ is the internal force constant and $s_{jk}^{\lambda}(\theta)$ is the internal coordinate given by $s_{jk}^{\lambda}(\theta)=B_{jk}(\theta)Mq^{\lambda}(\theta)$, where $B_{jk}(\theta)$ is the element of the B matrix corresponding to the jth connection in a particular harmonic motion. M is a matrix whose elements are $\delta_{ii'}/\sqrt{M_i}$ and $q^{\lambda}(\theta)$ is the matrix of eigenvectors corresponding to the frequency $\omega_\lambda(\theta)$.

Since we are primarily interested in the modes above 600 cm^{-1} where dispersion is small and valence bond motions are dominant, we need only to consider contributions at zone center frequencies ($\theta=0$). Therefore the character of a mode, for example, the λth band, can be made by looking for the largest $V_j^{\lambda}(0)$'s.

The PED function for the isolated daunomycin drug is given by

$$v_{jk}^{\sigma}=\frac{(s_{jk}^{\sigma})^{*}\phi_{jk}s_{jk}^{\sigma}}{\sum_{jk}(s_{jk}^{\sigma})^{*}\phi_{jk}s_{jk}^{\sigma}} \qquad (6)$$

in which ϕ_{jk} is the force constant and s_{jk}^{σ} is the internal coordinate given by $s_{jk}^{\sigma}=b_{jk}Mq^{\sigma}$ where b_{jk} is the element of the B matrix corresponding to a particular connection in a particular motion. M is a matrix whose elements are $\delta_{ii'}/\sqrt{M_i}$. q^{σ} is the matrix of eigenvectors corresponding to a particular frequency ω_σ.

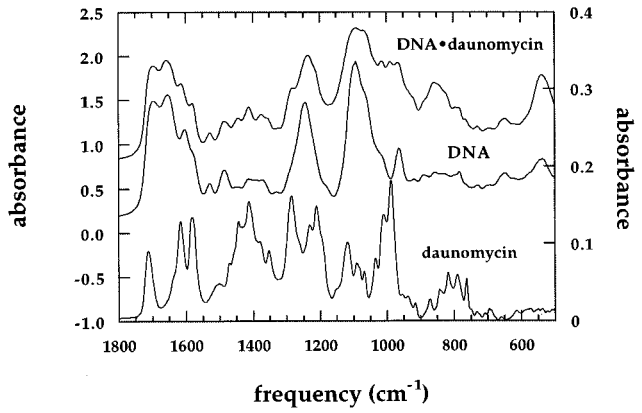

FIG. 2. The mid-infrared spectra of daunomycin, DNA, and the DNA·daunomycin complex. The samples were at 0% RH for all of the spectra. The scale on the left is for the DNA and the DNA·daunomycin complex. The spectrum of DNA·daunomycin has been shifted by 0.5 for convenience. The scale on the right is for daunomycin.

EXPERIMENTAL METHODS

Highly polymerized calf-thymus NaDNA was dissolved in 10-mM NaH_2PO_4 and 0.01-mM EDTA (ethylenediaminetetraacetic acid) buffer solution (pH=6.5). For the DNA·daunomycin complexes, DNA gels were saturated with daunomycin, resulting in samples with about one daunomycin for every four DNA base pairs. Free-standing films of DNA and DNA·daunomycin were prepared by placing a small amount of the gel on a Teflon block, which was then kept at a relative humidity (RH) of 75% for about 8 h. The block and film were then kept at 0% RH for about a day. This dessication caused the film to curl away from the block. The films were then mounted in a sealed sample chamber with ZnSe windows. Drierite was placed in the bottom of the sample chamber for dessication. Daunomycin samples were prepared in two different ways: a KBr pellet was made with daunomycin and a thin film of daunomycin was deposited on a Mylar sheet by evaporating a solution of daunomycin on the sheet. The spectra obtained from samples made by these two methods were identical.

Infrared spectroscopy was performed on the DNA·daunomycin samples at room temperature and 0% RH with two different Fourier transform infrared spectrometers: a Bruker 113v and a Nicolet SX-60. 300 scans of the sample and reference were taken. The spectra we present are unmodified; no Fourier deconvolutions or subtractions have been performed.

RESULTS AND DISCUSSIONS

Figure 2 shows the measured IR spectra for the DNA·daunomycin, free DNA and free daunomycin at 0% RH. The IR spectrum of the complex shows absorption features from both the DNA and the daunomycin. The DNA absorption features dominate the spectrum of the complex, mainly because there is only one daunomycin molecule for about every four DNA base pairs. Though the IR spectra for the DNA·daunomycin and DNA films have an overall similarity, there are several important differences that will be discussed below.

The calculated normal mode frequencies for the drug free poly d(CGTA)·poly d(TACG) above 600 cm^{-1} are given in Table I along with the assigned IR experimental frequencies for calf-thymus Na-DNA. The location of the largest PED's for the modes are also listed as well as the residue of the PED assignment. Normal mode frequencies for the daunomycin-bound poly d(CGTA)·poly d(TACG) are shown in Table II. In Table II the PED's of the drug-DNA complex are compared in the common degrees of freedom to find the modes that are of similar character in either the free DNA or the isolated daunomycin. The frequency differences between these modes and those in the free molecules are also displayed in Table II along with the measured IR frequency shifts. The last column in Table II lists the dominant residue in DNA for modes primarily in DNA and lists D for those primarily in daunomycin.

With the use of the mode assignments for the DNA·daunomycin complex given in Table II, a very tentative set of assignments for the isolated daunomycin is presented in Table III. The modes not assigned in Table II are assigned on the basis of frequency, which is very uncertain. In the present work the daunomycin valence force constants are from AMBER. These force constants were not refined to the vibrational spectrum of daunomycin. No attempt was made in the present work to further refine these force constants. The assignment of the daunomycin modes is therefore very tentative, based on these unrefined force constants. Nonetheless these force constants seem to give results in qualitative agreement with observations. This qualitative agreement is sufficient to yield information leading to a reasonable interpretation of the origin of the observed frequency shifts.

DNA modes

We find from Tables I and II that our calculated DNA frequencies for both free DNA and daunomycin-bound DNA are in fair agreement with the respective IR spectra. The frequencies for the calculated normal modes in the daunomycin-bound DNA are different from that in the free DNA but are similar to that in the IR spectra. There appears to be a well defined pattern in the frequency shifts. Large shifts are found in the modes primarily with localized motions in the sugar-phosphate groups near the binding site and in the $C2$-$N3$ and $C2$-$N2$ bonds in the two guanine bases adjacent to the drug. The frequency change for the modes localized in other regions of DNA are relatively small. This pattern of frequency shift is closely related to the structural features of the daunomycin-bound DNA crystal on which our model is constructed.

X-ray diffraction studies of DNA·daunomycin complexes [15–18] showed that the intercalation of the daunomycin planar aglycon group into the space between base pairs displaces the adjacent base pairs and unwinds the backbone. Although generally falling in the region of the B-conformation, the individual torsion angles in the backbones at the binding site are changed substantially to accommodate the drug planar group. In our DNA·daunomycin system the drug is intercalated between every $C1$-$G8$ and $G2$-$C7$ base pair. Substantial torsion angle change is found in the phosphate groups between $C1$ and $G2$ and between

TABLE I. Comparison between the observed IR frequency ω^{expt} for calf-thymus *B*-DNA and the calculated normal mode frequencies ω^{theor} for *B*-DNA poly *d*(CGTA)·poly *d*(TACG). The assignments of the modes are from the analysis of potential energy distribution (PED). Only those modes identified in the IR spectrum are given. The bases are labeled as *C*1-*G*2-*T*3-*A*4 in one strand and *G*8-*C*7-*A*6-*T*5 in the opposite strand.

IR ω^{expt} (cm^{-1})	ω^{theor} (cm^{-1})	Calculation Assignment (PED %)	Residue
1714	1682	*c*4-*o*4 (47.3), *c*5-*c*4 (14.0), *c*2-*o*2 (14.0)	*T*3, *T*5
1665	1656	*c*6-*o*6 (52.8), *c*5-*c*6 (17.6), *c*5-*c*4 (17.6)	*G*2, *G*8
1610	1606	*c*5-*c*4 (46.5), *c*5-*c*6 (22.1), *n*3-*c*4 (22.1)	*A*4, *A*6
1578	1606	*c*5-*c*4 (46.5), *c*5-*c*6 (22.1), *n*3-*c*4 (22.1)	*A*6, *A*4
1529	1539	*c*4-*n*9 (30.6), *c*5-*c*6 (9.9), *n*3-*c*4 (9.9)	*G*8, *G*2
1505	1494	*n*3-*c*2 (17.0), *c*4-*n*3 (13.4), *c*2-*n*1 (13.4)	*C*1, *C*7
1488	1485	*c*5-*c*4 (31.4), *c*4-*n*3 (25.3), *c*5-*Me* (25.3)	*T*3, *T*5
1481	1483	*c*4-*n*9 (44.5), *n*3-*c*4 (8.4), *c*5-*c*6 (8.4)	*A*6, *A*4
1427	1432	*c*2-*n*1 (34.3), *n*3-*c*2 (19.4), *c*6-*c*5 (19.4)	*T*3, *T*5
1418	1430	*c*6-*n*1 (34.7), *c*6-*n*6 (22.5), *n*1-*c*2 (22.5)	*A*4, *A*6
1392	1413	*c*2-*n*3 (44.5), *c*2-*n*2 (25.8), *n*2-*c*2-*n*1 (25.8)	*G*8, *G*2
1377	1405	*n*1-*c*2 (24.3), *n*7-*c*5 (13.0), *c*4-*n*9 (13.0)	*G*2, *G*8
1373	1367	*c*4-*n*4 (29.8), *c*6-*c*5 (13.3), *c*2-*n*1 (13.3)	*C*1, *C*7
1329	1329	*n*1-*c*6 (32.3), *c*5-*Me* (19.3), *c*1*-*n*1 (19.3)	*T*3, *T*5
1304	1323	*c*2-*n*3 (29.8), *n*1-*c*2 (23.6), *c*6-*n*6 (23.6)	*A*4, *A*6
1243	1244	*c*6-*c*5 (18.4), *n*1-*c*6 (13.3), *n*3-*c*2 (13.3)	*C*1, *C*7
1278	1269	*o*4*-*c*1* (27.9), *c*4*-*o*4* (24.9), *o*4*-*c*1*-*c*2* (24.9)	*C*1, *T*3
1248	1234	*c*1*-*n*1 (16.5), *c*4-*n*3 (7.4), *c*2-*n*1 (7.4)	*T*3, *T*5
1211	1210	*p*-*o*1 (28.8), *p*-*o*2 (27.5)	*G*2-*T*3, *T*3-*A*4
1182	1160	^{1}*c*4*-*o*4* (7.3), ^{2}*n*3-*c*4 (4.7), ^{1}*o*4*-*c*1* (4.7)	^{1}*A*6, ^{2}*G*8
1142	1152	*c*4*-*o*4* (10.3), *c*4-*n*3 (9.4), *n*3-*c*2 (9.4)	*T*3
1097	1108	^{1}*p*-*o*2 (28.1), ^{1}*p*-*o*1 (19.9), ^{2}*c*5*-*o*5* (19.9)	^{1}*T*5-*G*8, ^{2}*A*6-*C*7
1094	1105	^{1}*p*-*o*2 (25.7), ^{1}*p*-*o*1 (22.3), ^{2}*p*-*o*2 (22.3)	^{1}*G*2-*C*1, ^{2}*T*3-*G*2
1094	1102	*p*-*o*2 (41.1), *p*-*o*1 (39.4), *o*2-*o*1 (39.4)	*G*8-*C*7, *A*4-*C*1
1078	1082	^{1}*o*5*-*c*5* (38.6), ^{2}*c*4*-*o*4* (11.4), ^{2}*c*1*-*c*2* (11.4)	^{1}*G*2-*C*1, ^{2}*T*3
1078	1080	^{1}*c*5*-*o*5 (10.7), ^{2}*c*5*-*o*5 (8.8), ^{3}*c*1*-*c*2* (8.8)	^{1}*A*6-*C*7, ^{2}*G*8-*T*5 ^{3}*G*8
1052	1053	*c*1*-*c*2* (11.1), *c*1*-*c*2* (6.6)	*T*3, *T*5, *A*6
1008	1016	*c*1*-*c*2* (11.6), *n*1-*c*2 (6.4), *c*2-*n*2 (6.4)	*G*2
960	954	*o*4*-*c*1* (9.8), *c*1*-*c*2* (8.1), *c*5-*Me* (8.1)	T3
857	860	^{1}*o*3-*p* (10.0), ^{2}*c*1*-*c*2*-*c*3* (5.5), ^{2}*c*2*-*c*3*-*c*4* (5.5)	^{1}*G*8-*C*7, ^{2}*C*7
802	795	*n*1-*c*6-*c*5 (7.6), *c*5-*c*4 (7.6)	*T*3,*T*5
779	757	*c*4-*n*4 (10.2), *n*1-*c*6-*c*5 (9.5), *c*6-*c*4 (9.5)	*C*1, *C*7
766	753	*c*1*-*c*2*-*c*3* (13.6), *o*4*-*c*1*-*c*2* (7.8), *c*3*-*c*4* (7.8)	*T*3, *T*5
732	751	^{1}*c*1*-*c*2*-*c*3* (7.9), ^{1}*c*2*-*c*3*-*c*4* (4.7), ^{2}*c*3*-*o*3-*p* (4.7)	^{1}*G*8, ^{2}*A*6-*T*5
726	723	*c*1*-*c*2*-*c*3* (9.2), *o*4*-*c*1*-*c*2* (5.6), *o*4*-*c*1* (5.6)	*G*8
717	707	*c*3*-*c*4*-*o*4*(17.9), *c*2*-*c*3*-*c*4*(13.4), *c*4*-*o*4**c*1*(13.4)	*C*1, *C*7
694	686	*n*1-*c*2-*o*2 (7.9) *c*4-*c*5-*Me* (7.2)	*T*3, *T*5
666	664	*o*4*-*c*1*-*c*2* (12.6), *c*1*-*n*1 (10.8)	*C*1, *C*7
663	622	*o*4*-*c*1*-*n*9 (5.9), *c*2*-*c*3*-*o*3 (5.9)	*A*6
650	641	*Me*-*c*4-*c*6-*c*5 (12.3), *c*2*-*c*3*-*o*3 (7.8)	*T*3

*C*7 and *G*8. Substantial torsion angle change is also found in the phosphate groups between *G*2 and *T*3, *C*7 and *A*6, *C*1 and *A*4 in a neighboring unit cell, and *G*8 and *T*5 in a neighboring unit cell. In addition, torsion angle change is also observed in the sugar group connected to the *C*1, *G*2, *C*7, and *G*8 bases. Such a structural change is expected to induce substantial change in the partition of the harmonic restoring force in the normal mode coordinates associated with the vibrational motion in the region. We find from Table II that, except for two modes associated with guanine *C*2-*N*3 and *C*2-*N*2 bonds, all DNA modes with large frequency shift (more than 10 cm^{-1}) are in these sugar-phosphate groups.

Apart from the specified backbone modes, there are two modes, corresponding to an experimental IR line at 1375 cm^{-1}, that show large frequency shift. These two modes are primarily localized in the *C*2-*N*3 and *C*2-*N*2 bonds in the *G*2 and *G*8 base, respectively. The frequency shift in these modes occurs because of the change in the relative position of the *N*3 and *N*2 atoms in these bases in the

TABLE II. Comparison between the observed IR frequencies ω^{expt} of daunomycin-bound calf-thymus DNA and the calculated normal mode frequencies ω^{theor} for daunomycin-bound poly d(CGTA)·poly d(TACG). $\Delta\omega^{\text{expt}}$ and $\Delta\omega^{\text{theor}}$ are the difference between the frequency of the drug-DNA system and that of the free drug or DNA molecule from experiments and from our calculation, respectively. The assignments of the modes are from the analysis of potential energy distribution (PED). Only those modes identified in the IR spectrum are given. The bases are labeled as *C*1-*G*2-*T*3-*A*4 in one strand and *G*8-*C*7-*A*6-*T*5 in the opposite strand.

IR		Calculation			
ω^{expt} (cm^{-1})	$\Delta\omega^{\text{expt}}$ (cm^{-1})	ω^{theor} (cm^{-1})	$\Delta\omega^{\text{theor}}$ (cm^{-1})	Assignment (PED %)	Residue
1705	−9	1738	−3	*c*12-*o*12 (18.7), *c*5-*o*5 (15.7), *c*12-*c*15 (15.7)	*D*
1658	−7	1649	−8	*c*6-*o*6 (51.5), *c*5-*c*6 (19.3), *c*5-*c*4 (19.3),	*G*2
1617	7	1608	2	*c*5-*c*4 (44.8), *c*5-*c*6 (24.0), *n*3-*c*4 (24.0)	*A*4; *A*6
1579	−3	1591	−12	*c*6-*c*20 (14.2), *c*5-*o*5 (12.4), *c*19-*c*11 (12.4)	*D*
1529	0	1540	1	*c*4-*n*9 (28.9), *c*5-*c*4 (17.5), *c*6-*o*6 (17.5),	*G*2
1491	3	1490	5	*c*5-*c*4 (32.8), *c*4-*n*3 (26.1), *c*5-*Me* (26.1),	*T*3
1447	−3	1453	−4	*c*19-*c*11 (15.8), *c*20-*c*19 (15.8), *c*20-*c*7 (15.8),	*D*
1414	−4	1424	−6	*c*6-*n*1 (34.6), *c*6-*n*6 (21.8), *n*1-*c*2 (21.8),	*A*4,*A*6
1375	−17	1402	−11	*c*2-*n*3 (33.0), *c*2-*n*2 (26.1), *n*9-*c*8 (26.1),	*G*2
1375	−17	1397	−16	*c*2-*n*3 (30.3), *c*2-*n*2 (28.4), *n*9-*c*8 (28.4),	*G*8
1357	3	1335	0	*c*12-*o*12 (18.2), *c*17-*c*18 (14.7), *c*6-*o*6 (14.7),	*D*
1325	−4	1326	−3	*n*1-*c*6 (34.7), *c*5-*Me* (19.4), *c*1*-*n*1 (19.4)	*T*3,*T*5
1284	6	1275	6	*o*4*-*c*1* (27.0), *c*4*-*o*4* (26.9), *c*2*-*c*3*-*c*4* (26.9)	*T*3,*T*5
1238	−5	1239	−5	*c*6-*c*5 (21.2), *n*1-*c*6 (15.6), *n*3-*c*2 (15.6)	*C*1
1094	16	1096	16	^{1}*c*5*-*o*5* (13.3), ^{2}*c*1*-*c*2* (12.9), ^{2}*c*3*-*c*4* (12.9)	^{1}*A*6-*C*7, ^{2}*G*8
1094	16	1091	11	^{1}*c*5*-*o*5* (14.8), ^{2}*c*5*-*o*5* (12.9), ^{1}*p*-*o*2 (12.9)	^{1}*C*7-*G*8, ^{2}*A*6-*C*7
1071	−26	1078	−30	^{1}*p*-*o*2 (31.4), ^{1}*p*-*o*1 (26.9), ^{2}*p*-*o*2 (26.9)	^{1}*T*5-*G*8, ^{2}*C*7-*G*8
1071	−23	1077	−25	^{1}*p*-*o*2 (22.5), ^{1}*p*-*o*1 (22.4), ^{2}*p*-*o*2 (22.4)	^{1}*C*7-*G*8, ^{2}*T*5-*G*8
1071	−23	1076	−29	*p*-*o*2 (33.3), *p*-*o*1 (28.1), *o*5*-*c*5* (28.1)	*G*2-*C*1
1058	−26	1060	−22	^{1}*o*5*-*c*5* (19.3), ^{2}*c*1*-*c*2* (10.4), ^{3}*p*-*o*2 (10.4)	^{1}*G*2-*C*1, ^{2}*T*3, ^{3}*A*4-*C*1
1015	−23	1045	−7	*c*4*-*o*4* (64.9), *c*5*-*o*5* (10.9), *c*5*-*c*6* (10.9)	*D*
986	−24	974	−8	*c*13-*c*14 (12.2), *c*7-*o*7 (11.3), *c*9-*c*10 (11.3)	*D*
971	−17	950	−4	*c*6-*o*6 (13.0), *c*11-*o*11 (9.6), *c*13-*c*14 (9.6)	*D*
890	−28	882	−33	*c*5*-*c*6* (22.1), *c*4*-*c*5* (18.4), *c*5*-*o*5* (18.4)	*D*
839	−18	843	−17	^{1}*o*3-*p* (35.2), ^{2}*c*2*-*c*3*-*o*3 (7.4), ^{2}*c*3*-*c*4* (7.4)	^{1}*G*8-*C*7, ^{2}*C*7-*A*6
796	−6	793	−2	*c*5-*c*4 (6.7), *n*1-*c*6-*c*5 (6.7)	*T*3,*T*5
763	−3	752	−1	*c*1*-*c*2*-*c*3* (9.7), *c*3*-*c*4* (9.4), *o*4*-*c*1*-*c*2* (9.4)	*T*3,*T*5
730	−2	744	−7	^{1}*c*2*-*c*3*-*c*4* (11.6), ^{2}*o*5-*p* (8.2), ^{3}*o*5-*p* (8.2)	^{1}*G*8, ^{2}*G*8-*C*7, ^{3}*T*5-*G*8
707	−10	694	−13	*c*3*-*c*4*-*o*4*(14), *c*2*-*c*3*-*c*4*(11), *c*1*-*c*2*-*c*3*(11)	*C*1,*C*7
696	2	689	3	*n*1-*c*2-*o*2 (8.8), *c*4-*c*5-*Me* (8.8)	*T*3,*T*5
658	−8	651	−13	*o*4*-*c*1*-*c*2* (6.6), *o*2-*c*2-*n*1 (6.5)	*C*1
643	−7	635	−6	*Me*-*c*4-*c*6-*c*5(25), *c*2*-*c*3*-*o*3(7), *c*3*-*c*4*-*o*4*(7)	*T*3

DNA·daunomycin crystal. This position change results from the formation of H bonds between these atoms and the drug in the crystal. Crystal x-ray analysis [16,17] showed that direct drug-base H bonds are formed between the drug *O*9 atom and the *N*2 and *N*3 atoms in the *G*2 base, respectively, as shown in Fig. 3. The agreement between calculated and observed frequency shift seems to suggest that at least the formation of the direct drug-base H bonds is related to the observed IR frequency shift from 1392 cm^{-1} in free DNA to 1375 cm^{-1} in daunomycin-bound DNA.

As shown in Table II the remaining DNA modes, those not in the backbone at the binding site and in the *C*2-*N*3 and *C*2-*N*3 bonds in the guanine bases, have relatively small frequency change (less than 10 cm^{-1}) upon binding. The small frequency change in these modes is indicative of insignificant structural variation in the region of DNA helix excluding the backbone at the binding site and that of the *C*2-*N*3 and *C*2-*N*2 bonds of the guanine base. This is in good agreement with observed structural features in the crystal x-ray measurements. Experiments on several DNA·daunomycin crystal showed that no significant conformation change occurs in these regions of DNA helix [15–18]. Consequently the vibrational modes localized in these regions are not expected to show significant change by the binding of daunomycin.

Daunomycin modes

From Tables II and Table III we find that the calculated frequency and frequency shift for the daunomycin modes are in qualitative agreement with the observed IR spectra. The exact values of the calculated frequency shifts, however, differ to some extent from observed values. This discrepancy arises because of the use of unrefined daunomycin force con-

TABLE III. Comparison between the observed IR frequencies ω^{expt} and the calculated normal mode frequencies ω^{theor} for a free daunomycin crystal. The assignments of the modes are from the analysis of potential energy distribution (PED). Only those modes identified in the IR spectrum are given.

IR ω^{expt} (cm^{-1})	ω^{theor} (cm^{-1})	Calculation Assignment (PED %)
1714	1741	*c*12-*o*12 (20.4), *c*5-*o*5 (14.9), *c*12-*c*15 (9.5)
1619	1626	*c*3-*c*4 (26.0), *c*2-*c*3 (21.2), *c*1-*c*2 (13.3)
1582	1603	*c*6-*c*20 (17.3), *c*6-*o*6 (14.4), *c*19-*c*11 (14.0)
1450	1457	*c*20-*c*7 (16.6), *c*20-*c*19 (16.4), *c*6-*c*20 (12.5)
1412	1437	*c*9-*c*13 (43.1), *c*13-*c*14 (20.0), *c*8-*c*9 (7.1)
1360	1335	*c*12-*o*12 (18.2), *c*17-*c*18 (13.5), *c*6-*o*6 (11.9)
1284	1261	*c*8-*c*9 (30.0), *c*7-*c*8 (20.3), *c*9-*c*10 (12.1)
1209	1214	*c*9-*o*9 (25.6), *c*9-*c*10 (17.9), *c*16-*c*15 (4.6)
1117	1118	*o*7-*c*1* (28.7), *c*7-*c*8 (14.2), *c*5*-*c*6* (7.8)
1038	1052	*c*4*-*o*4* (35.1), *c*5*-*o*5* (21.5), *c*5*-*c*6* (10.8)
1010	982	*c*7-*o*7 (16.9), *c*13-*c*14 (11.5), *c*8-*c*9 (7.2)
988	954	*c*6-*o*6 (18.2), *c*11-*o*11 (12.6), *c*17-*c*6 (6.2)
918	915	*c*2*-*c*3* (20.3), *c*5*-*c*6* (16.9), *c*3*-*n*3* (15.9)
844	843	*o*5*-*c*1* (27.3), *o*7-*c*1* (16.9), *c*4*-*o*4* (12.7)
818	830	*c*15-*c*1-*c*2 (11.3), *c*1-*c*2-*c*3 (8.2), *c*11-*c*18-*c*12 (7.5)
790	765	*c*4*-*o*4* (18.3), *c*4*-*c*5* (17.6), *c*3*-*c*4* (12.5)
763	740	*c*1-*c*2-*c*3 (13.8), *c*15-*c*1-*c*2 (8.5), *c*8-*c*9 (7.4)

stants in our calculation. We expect this discrepancy to diminish with the use of a set of refined force constants. Nonetheless the qualitative agreement is sufficient to propose the character of the IR lines and thus interpret the observed frequency shift for daunomycin modes.

We find from Table II a distinctive pattern in the observed IR frequency shift for daunomycin modes. As shown in Table II large IR frequency shift is found for the modes with localized motion in certain bonds of ring *A* (see Fig. 1) in the aglycon chromophore (*C*13-*C*14, *C*7-*O*7, *C*9-*C*10, *C*6-*O*6, and *C*11-*O*11 bonds) and in certain bonds in the amino-sugar group (*C*5*-*O*4*, *C*5*-*C*6*, *C*5*-*O*5*, and *C*4*-*C*5* bonds) of the drug. Crystal x-ray analysis showed that the conformation of these bonds is altered because of deformation as a result of its binding to DNA [16]. This conformation change is therefore expected to result in significant frequency shift in the modes localized in these regions of the drug. All the remaining daunomycin modes in Table II are found to have relatively small IR frequency shift. These modes correspond to vibrational modes localized in the regions with no significant structural variation upon binding. It is therefore not surprising to find small frequency shift in these modes.

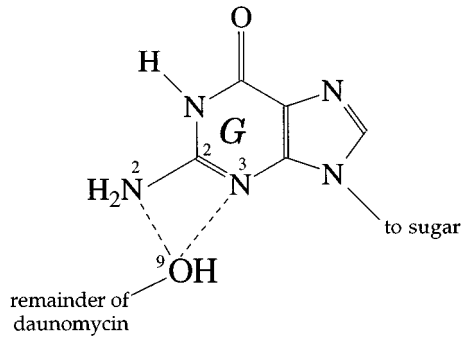

FIG. 3. The atoms involved in the guanine-daunomycin interaction.

The agreement between observed frequency shift and observed structural feature of binding indicates the correlation between structure and vibrational spectra. On the other hand it also serves to confirm the validity of our mode assignment for daunomycin modes even though unrefined force constants are used for the daunomycin drug in our calculation.

ORIGIN OF FREQUENCY SHIFT

Our studies in an earlier work [11] and in the present work indicate that the dominant factor for the observed significant frequency shift in a drug-DNA complex is the conformation deformation induced by drug binding. Structural deformation affects vibrational spectra by alteration of the partition of harmonic restoring forces in different normal mode coordinates. This can be easily understood from Eq. (3) and Eq. (4). From these equations one finds that vibrational frequencies depend on the transformation matrix as well as the force fields. The transformation matrix or *B* matrix is a matrix that links the internal coordinates to the mass weighted Cartesian coordinates. The elements of this matrix are dependent on the structure of the molecule. Conformation deformation therefore leads to a change in these elements. Consequently the partition of the force fields (the harmonic restoring forces) into different normal mode coordinates is altered. This alteration then leads to the shift in the normal mode frequencies.

In our calculation the same set of valence force constants is used in both the free molecules and in the drug-bound system. In addition to these valence force constants we have introduced nonbonded force constants into our dynamical

TABLE IV. Comparison between the DNA normal mode frequencies of poly d(CGTA)·poly d(TACG) bound by daunomycin, the free deformed DNA helix with the same conformation as that bound by daunomycin, and the free B-conformation helix.

Drug bound		Deformed		Free		
ω (cm^{-1})	First assignment (PED %)	ω (cm^{-1})	First assignment (PED %)	ω (cm^{-1})	First assignment (PED %)	Residue
1676	*c*4-*o*4(44)	1676	*c*4-*o*4(44)	1682	*c*4-*o*4(47)	*T*3,*T*5
1649	*c*6-*o*6(52)	1649	*c*6-*o*6(46)	1656	*c*6-*o*6(52)	*G*2
1608	*c*5-*c*4(45)	1610	*c*5-*c*4(45)	1606	*c*5-*c*4(47)	*A*4
1540	*c*4-*n*9(29)	1540	*c*4-*n*9(29)	1539	*c*4-*n*9(31)	*G*2
1490	*c*5-*c*4(33)	1490	*c*5-*c*4(33)	1485	*c*5-*c*4(31)	*T*3
1424	*c*6-*n*1(35)	1426	*c*6-*n*1(34)	1430	*c*6-*n*1(35)	*A*4,*A*6
1402	*c*2-*n*3(33)	1402	*c*2-*n*3(33)	1413	*c*2-*n*3(45)	*G*2
1397	*c*2-*n*3(30)	1404	*c*2-*n*3(28)[a]	1413	*c*2-*n*3(45)	*G*8
1326	*n*1-*c*6(35)	1326	*n*1-*c*6(35)	1329	*n*1-*c*6(32)	*T*3,*T*5
1275	*o*4*-*c*1*(27)	1275	*o*4*-*c*1*(27)	1269	*o*4*-*c*1*(28)	*T*3
1239	*c*6-*c*5(21)	1240	*c*6-*c*5(21)	1244	*c*6-*c*5(18)	*C*1
1096	*c*1*-*c*2*(13)[a]	1097	*c*1*-*c*2*(20)	1080	*c*1*-*c*2*(9)[a]	*G*8
1091	*c*5*-*o*5*(13)[a]	1092	*c*5*-*o*5*(22)	1080	*c*5*-*o*5(11)	*A*6-*C*7
1078	*p*-*o*2(31)	1078	*p*-*o*2(36)	1108	*p*-*o*2(28)	*T*5-*G*8
1077	*p*-*o*2(23)	1077	*p*-*o*2(27)	1102	*p*-*o*2(41)	*C*7-*G*8
1076	*p*-*o*2(33)	1076	*p*-*o*2(34)	1105	*p*-*o*2(26)	*G*2-*C*1
1060	*o*5*-*c*5*(19)	1060	*o*5*-*c*5*(18)	1082	*o*5*-*c*5*(39)	*G*2-*C*1
843	*o*3-*p*(35)	842	*o*3-*p*(35)	860	*o*3-*p*(10)	*G*8-*C*7
793	*c*5-*c*4(7)	793	*c*5-*c*4(8)	795	*n*1-*c*6-*c*5(8)	*T*3,*T*5
752	*c*1*-*c*2*-*c*3*(10)	752	*c*1*-*c*2*-*c*3*(10)	753	*c*1*-*c*2*-*c*3*(14)	*T*3,*T*5
744	*c*2*-*c*3*-*c*4*(12)	737	*c*2*-*c*3*-*c*4*(9)	751	*c*2*-*c*3*-*c*4*(5)[a]	*G*8
694	*c*3*-*c*4*-*o*4*(14)	694	*c*3*-*c*4*-*o*4*(15)	707	*c*3*-*c*4*-*o*4*(18)	*C*1,*C*7
689	*n*1-*c*2-*o*2(9)	689	*n*1-*c*2-*o*2(9)	686	*n*1-*c*2-*o*2(8)	*T*3,*T*5
651	*o*4*-*c*1*-*c*2*(7)	652	*o*4*-*c*1*-*c*2*(10)[a]	664	*o*4*-*c*1*-*c*2*(13)	*C*1
635	*Me*-*c*4-*c*6-*c*5(25)	635	*Me*-*c*4-*c*6-*c*5(25)	641	*Me*-*c*4-*c*6-*c*5(12)	*T*3

[a]Case where the character of the mode with largest PED is different from that in the other system, the mode with second or third largest PED is used for comparison.

force field to describe the effect of van der Waals and Coulomb interactions on the vibrational motions in molecules. The conformation change induced by drug binding results in the change in the intramolecular nonbonded force constants. Additional intermolecular nonbonded force constants and drug-base H-bond force constants also arise in the drug-DNA system. As a result the force constant matrix is modified. The nonbonded and H-bond force constants are substantially smaller than valence force constants. The modification is comparable to the valence force field only for molecules with drastic deformation or molecules with close and extensive contact with a large molecule. For small force field modifications the vibrational frequencies above 600 cm^{-1} will hardly change since the modes in these regions are predominantly valence bond vibrations. Large modifications will, however, have a sizable effect on the frequencies in this region, as seen by the 17-cm^{-1} shift of the 1392-cm^{-1} mode of free DNA.

To examine to what extent this force field modification contributes to the frequency shift in our DNA·daunomycin system, we carry out a calculation to determine the normal mode frequencies of a deformed free DNA and those of a deformed free daunomycin. These deformed free molecules are assumed to have the same conformation as in the complex. The normal modes determined in this manner have structural deformation but without the force field modification. The calculation is then compared to that of the drug-DNA complex, in which both deformation and force field modification is present, and to that of the free molecules, which have no deformation and are without force field modification. The frequencies and the first assignments (with largest PED percentage) of the modes of the deformed free DNA are given in Table IV along with the those of the DNA modes in the DNA·daunomycin complex and those in the free DNA. We find from Table IV that both the frequencies and the PED percentages of the DNA modes in the deformed free DNA are very close to those in the DNA·daunomycin complex. For most modes the frequency and PED percentage are essentially identical. This indicates that the modification to the DNA force field induced by daunomycin binding is relatively small, although DNA bases adjacent to the binding drug are displaced and unwound. Compared to DNA, daunomycin is a relatively small molecule. Therefore, the nonbonded forces from daunomycin are not strong enough to alter the DNA force fields. In contrast many frequencies and PED percentages in the deformed free DNA are substantially different from those in the free DNA. This confirms that the dominant factor of the frequency shift in DNA modes is the

TABLE V. Comparison between the normal mode frequencies of daunomycin bound to poly d(CGTA)·poly d(TACG), a deformed free daunomycin with the same conformation as that bound to DNA, and free daunomycin.

DNA bound		Deformed		Free	
ω (cm^{-1})	First assignment (PED %)	ω (cm^{-1})	First assignment (PED %)	ω (cm^{-1})	First assignment (PED %)
1738	$c12$-$o12$(19)	1734	$c12$-$o12$(19)	1741	$c12$-$o12$(20)
1591	$c6$-$c20$(14)	1594	$c6$-$c20$(17)	1603	$c6$-$c20$(17)
1453	$c20$-$c19$(16)[a]	1460	c20-c19(17)	1457	$c20$-$c19$(16)[a]
1335	$c12$-$o12$(18)	1335	$c12$-$o12$(18)	1335	$c12$-$o12$(18)
1268	$c8$-$c9$(31)	1280	$c8$-$c9$(40)	1261	$c8$-$c9$(30)
1045	$c4$*-$o4$*(65)	1046	$c4$*-$o4$*(54)	1052	$c4$*-$o4$*(35)
974	$c13$-$c14$(12)	965	$c13$-$c14$(10)	982	$c13$-$c14$(12)[a]
950	$c6$-$o6$(13)	943	$c6$-$o6$(8)	954	$c6$-$o6$(18)
882	$c5$*-$c6$*(22)	892	$c5$*-$c6$*(17)	915	$c5$*-$c6$*(17)[a]

[a]Case where the character of the mode with largest PED is different from that in the other system, the mode with second or third largest PED is used for comparison.

structural deformation induced by daunomycin binding.

Table V lists the frequencies and the first assignments for the modes of the deformed daunomycin along with those of the daunomycin modes in the DNA·daunomycin complex and those in the free daunomycin. Several modes in the deformed drug are found to be different in frequency from their counterparts in the DNA·daunomycin complex by several cm^{-1}. The use of unrefined force constants for daunomycin is not expected to contribute to such a frequency difference. Although the frequency changes are no more than several cm^{-1}, the occurrence of such changes indicates that the nonbonded interaction between daunomycin and DNA has some contribution to the dynamical force field of daunomycin. The binding of daunomycin places the drug aglycon chromophore group in a pocket formed by surrounding DNA bases and backbones. The strong nonbonded pocket interaction at certain regions of the binding drug then leads to the modification of the dynamical force field in the region, which in turn changes the frequency for the modes localized in these regions. Our study therefore indicates that nonbonded forces between a large molecule and a small molecule alter the dynamical force fields of the smaller molecule more significantly than that of the larger molecule.

CONCLUSION

High frequency vibrational modes correspond to highly localized vibrational motions in molecules. These modes are sensitive to structural deformation and they can be used to probe the sites and types of deformation. The frequency shifts in the normal modes of DNA and daunomycin induced by the binding of these two molecules show clear correlation between frequency and the structural deformation revealed by crystal x-ray analysis. Substantial frequency shift occurs in the modes associated with localized vibrational motions in regions of DNA and the drug where most structural deformation takes place. In contrast, the modes correlated to the regions where no significant structural change occurs show only minor frequency shift. The frequency shift in our DNA·daunomycin system originates primarily from the change in the partition of the harmonic restoring forces in the normal mode coordinates induced by deformation. Although deformation also results in the change in the nonbonded interactions, this change appears to have relatively small effect on DNA dynamical force fields. It does have some effect on the force field of the drug confined by the DNA. The correlation between frequency and structure probed by the present work has potential application in identification of sites and types of deformation in biomolecules from Raman and IR spectra. Further theoretical investigation is needed to establish quantitative correlation between frequency and specific structural deformations in various biomolecules so that enough knowledge can be gained to achieve the above objective.

ACKNOWLEDGMENTS

This work is supported in part by ONR Grant N00014-92-K-1232 and a grant to Reed College under the Howard Hughes Medical Institute Undergraduate Biological Sciences Initiative.

[1] E. Taillandier and J. Liquier, Methods Enzym. **211**, 307 (1992).

[2] W.L. Peticolas and E. Evertsz, Methods Enzym. **211**, 335 (1992).

[3] K.C. Lu, E.W. Prohofsky, and L.L. Van Zandt, Biopolymers **16**, 2491 (1977).

[4] R. Letellier, M. Ghomi, and E. Thaillandier, J. Biomol. Struct. Dyn. **3**, 671 (1986).

[5] Y. Guan, C.J. Wurrey, and G.J. Thomas, Jr., Biophys. J. **66**, 225 (1994).
[6] E.W. Small and W.L. Peticolas, Biopolymers **10**, 1377 (1971).
[7] T. Thamann, R.C. Lord, A.H.-J. Wang, and A. Rich, Nucleic Acids Res. **9**, 5443 (1981).
[8] Y. Nishimura, M. Tsuboi, T. Nakano, S. Higuchi, T. Sato, T. Shida, S. Uesugi, E. Ohtsuka, and M. Ikehara, Nucleic Acids Res. **11**, 1579 (1983).
[9] G.J. Thomas, Jr., J.M. Benevides, and B. Prescott, Biomol. Stereodyn. **4**, 227 (1986).
[10] J.M. Benevides, A.H.-J. Wang, G.A. van der Marel, J.H. van Boom, and G.J. Thomas, Jr., Biochemistry **27**, 931 (1988).
[11] Y.Z. Chen and E.W. Prohofsky, Biopolymers **35**, 657 (1995).
[12] S.A. Lee, B. Sclavi, J.W. Powell, W. Williamson III, and A. Rupprecht, Phys. Rev. E **48**, 2240 (1993).
[13] A. DiMarco, F. Arcamone, and F. Zunino, in *Antibiotics, Mechanism of Action of Antimicrobial and Antitumor Agents*, edited by J.W. Corcoran and F.E. Hahn (Springer-Verlag, Berlin, 1975), p. 101.
[14] S. Neidle and G. Taylor, Biochim. Biophys. Acta **478**, 450 (1977).
[15] G.J. Quigley, A.H.-J. Wang, G. Ughetto, G. van der Marel, J.H. van Boom, and A. Rich, Proc. Natl. Acad. Sci. USA **77**, 7204 (1980).
[16] A.H.-J. Wang, G. Ughetto, G.J. Quigley, and A. Rich, Biochemistry **26**, 1152 (1987).
[17] C.A. Frederick, L.D. Williams, G. Ughetto, G.A. van der Marel, J.H. van Boom, A. Rich, and A.H.-J. Wang, Biochemistry **29**, 2538 (1990).
[18] C.M. Nunn, L.V. Meervelt, S. Zhang, M.H. Moore, and O. Kennard, J. Mol. Biol. **222**, 167 (1991).
[19] D.R. Phillips, A. Dimarco, and F. Zunino, Eur. J. Biochem. **85**, 487 (1978).
[20] J.B. Chaires, N. Dattagupta, and D.M. Crothers, Biochemistry **21**, 3933 (1982).
[21] D.P. Remeta, C.P. Mudd, R.L. Berger, and K.J. Breslauer, Biochemistry **32**, 5064 (1993).
[22] K.X. Chen, N. Gresh, and B. Pullman, J. Biomol. Struct. Dyn. **3**, 445 (1985).
[23] P. Cieplak, S.N. Rao, P.D.J. Grootenhus, and P.A. Kollman, Biopolymers **29**, 717 (1990).
[24] Y.Z. Chen and E.W. Prohofsky, Biophys. J. **66**, 820 (1994).
[25] Y.Z. Chen and E.W. Prohofsky, Eur. Biophys. J **24**, 203 (1996).
[26] R. Chandrasekaran and S. Arnott, in *Crystallographic and Structural Data II*, edited by W. Saenger, Landolt-Börnstein, New Series, Group VII, Vol. 1, pt. a (Springer-Verlag, Berlin, 1989), p. 31.
[27] S. Califano, *Vibrational States* (John Wiley and Sons, New York, 1976).
[28] M. Tsuboi, S. Takahashi, and I. Harada, in *Physico-Chemical Properties of Nucleic Acids*, edited by J. Duchesne (Academic Press, New York, 1973), Vol. 2, p. 91.